Acta Crystallographica Section B
Structural Science
ISSN 0108-7681

Submolecular partitioning of morphine hydrate based on its experimental charge density at 25 K

S. Scheins, M. Messerschmidt and P. Luger*

Institut für Chemie/Kristallographie der Freien Universität Berlin, Takustrasse 6, Berlin D-14195, Germany

Correspondence e-mail: luger@chemie.fu-berlin.de

Received 18 January 2005
Accepted 23 May 2005

The electron density distribution of morphine hydrate has been determined from high-resolution single-crystal X-ray diffraction measurements at 25 K. A topological analysis was applied and, in order to analyze the submolecular transferability based on an experimental electron density, a partitioning of the molecule into atomic regions was carried out, making use of Bader's zero-flux surfaces to yield atomic volumes and charges. The properties obtained were compared with the theoretical calculations of smaller fragment molecules, from which the complete morphine molecule can be reconstructed, and with theoretical studies of another opiate, Oripavine PEO, reported in the literature.

1. Introduction

A substantial aspect of Bader's theory of atoms in molecules (AIM; Bader, 1994) is the partitioning of a molecule into submolecular or even atomic regions. A submolecular functional group is defined as a bounded region in real space given by the interatomic surface of zero flux in the gradient vector field of the electronic charge density $\rho(\mathbf{r})$. By integration over these zero-flux surfaces, group or atomic properties such as atomic volumes or charges can be derived.

Matta (2001) presented a method, based on theoretical calculations, of reconstructing larger molecules from submolecular fragments of a morphine-related oripavine derivative (PEO). The properties of the atoms in the fragment molecules were thereby summed to obtain the properties of the large molecule. Matta showed that because of the transferability and additivity of the atomic properties, the reconstruction of large complicated molecules from smaller fragments is a close approximation of the density of an intact molecule.

This procedure should be considered in light of the fact that the experimental charge density of large molecules or macromolecules is difficult to obtain since the crystal quality is in general not sufficient for such an elaborate experiment. The partitioning scheme is therefore a suitable instrument to overcome the problems presented with larger molecules.

For charge density work morphine can be considered as a medium-sized molecule. Since we were able to grow nicely diffracting crystals, an experimental charge density distribution could be determined which can be compared with appropriate submolecular fragments according to Matta's work, so that the theoretical findings can be compared with experimental evidence.

Therefore, the morphine molecule was divided into three fragments representing different parts of the complete mole-

cule. Fig. 1 shows the complete molecule as derived from the X-ray analysis at 25 K (top left, including the chosen atomic numbering scheme) and the three fragments used to build up the morphine molecule. The intensely colored atoms were compared with the experimental values, whereas the pale colored atoms simulate an electronic environment corresponding to that in the intact molecule.

2. Experimental

Commercial morphine hydrochloride was dissolved in water and an equimolar solution of sodium hydroxide was added. The solution was heated under reflux for 2 h, then cooled and the free base was filtered. The white powder of the free base was recrystallized by slow evaporation of a solution in ethanol/water. The X-ray data set was collected with Mo $K\alpha$ radiation (graphite monochromator) at 25 K on a large four-circle Eulerian cradle (Huber, type 512) equipped with a double-stage closed-cycle He cryostat (Displex, Air Products, USA), a new 0.1 mm Kapton-film vacuum chamber around the cold head and a Bruker-APEX area detector (Meserschmidt *et al.*, 2003). The measurement strategy was planned with *COSMO* and for the data collection and integration the *SMART* and *SAINT* routines (Bruker AXS Inc., 1997–2001) were used. There were 67 606 reflections which were measured up to a resolution of $\sin\theta/\lambda = 1.15$ Å^{-1} (or $d = 0.43$ Å) to give 9984 unique reflections. Further details on the crystal data and the experimental conditions are given in Table 1. The morphine hydrate structure known from the literature (Bye, 1976) was used for a spherical refinement which was performed with *SHELXL* (Sheldrick, 1997).

The spherical model was then used as input for the aspherical-atom multipole formalism (Hansen & Coppens, 1978) applied by the program package *XD* (Koritsánszky *et al.*, 2003). The octapolar level of the multipol population was used for C, N and O atoms, while bond-directed dipoles were applied for H atoms. Nine κ expansion/contraction parameters were refined additionally. To reduce the number of parameters local *m* symmetry was assigned to the C1, C2 and C3 atoms in the phenyl ring, and to C7 and C8 (sp^2 hybridized). The bond lengths to H atoms were set to the standard neutron distances (Allen *et al.*, 1992). Fig. 3 shows an experimental residual map of the adequate fit of the multipole model to the experimental data. An overall residual density ($-0.20 \leq \Delta\rho \leq 0.22$ e Å^{-3}) was found with the entire data set (*i.e.* with all the high-order data included) used for the residual density calculation at the end of the refinement.

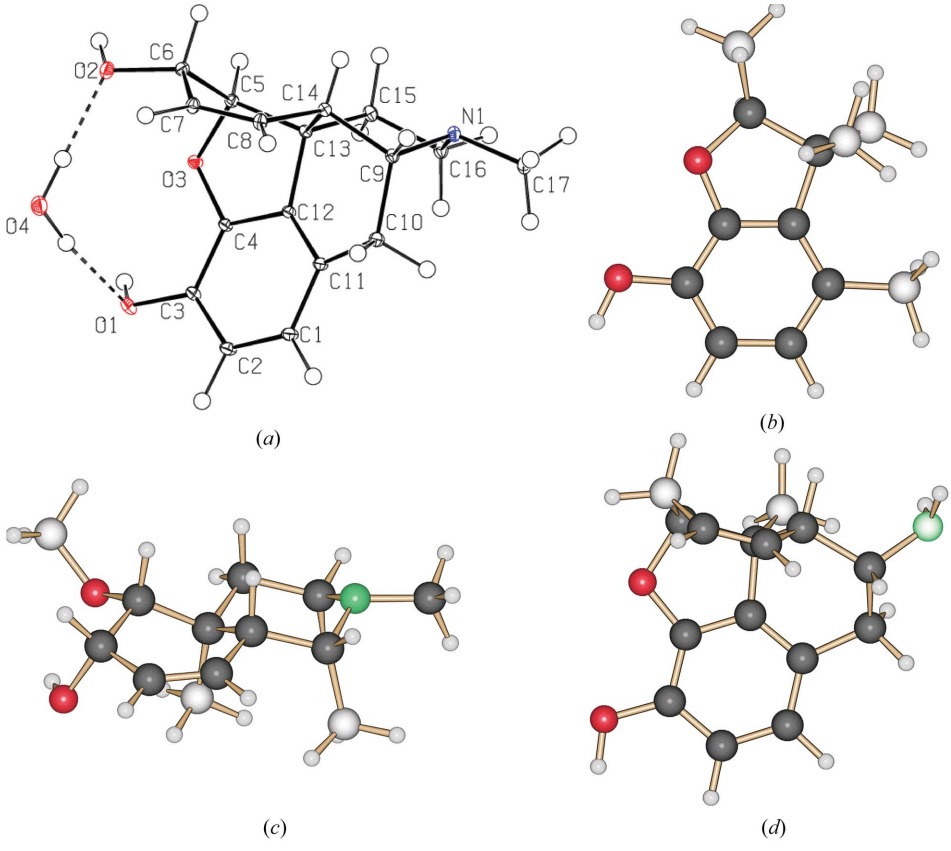

Figure 1
(*a*) The complete morphine molecule in an *ORTEP*III (Burnett & Johnson, 1996) representation (displacement ellipsoids at 25 K displayed at 50% probability; H atoms displayed at arbitrary radii) and (*b*)–(*d*) the three fragment molecules, including the atoms from which the morphine molecule can be built up. (*b*) Fragment 1 mimics the electron density of a benzofuranol molecule (rings *A* and *B*, see Fig. 2). (*c*) Fragment 2 emulates the electron density of the ring systems *D* and *E* and the ether oxygen. (*d*) Fragment molecule 3 mimics the electron density of the ring systems *A*, *C*, *D* and the C=C double bond.

3. Theoretical calculations

The *GAUSSIAN*98 program package (Frisch, 1998) was used for *ab initio* calculations at the density functional (B3LYP) level of theory. For the complete molecule the basis set 6-311++G(3df,3pd) was used for a single point calculation at the experimental geometry. The wavefunctions obtained were evalutated with the program package *AIMPAC* (Cheeseman *et al.*, 1992).

For the fragments a full energy optimization at the restricted Hartree–Fock (rHF) level and a 3-21g* basis set was performed. The optimized geometry was the subject of a single point SCF calculation at the rHF level using a 6-31G* basis set. This basis set was exactly the same as in Matta's study to allow a direct comparison with his theoretical results. To obtain the atomic properties of the fragment molecules the program *MORPHY*98 (Popelier & Bone, 1998) was used for the atomic integrations.

Table 1
Crystal data and structure refinement for morphine hydrate.

Crystal data	
Chemical formula	$C_{17}H_{19}NO_3{\cdot}H_2O$
M_r	303.35
Cell setting, space group	Orthorhombic, $P2_12_12_1$
a, b, c (Å)	7.431 (6), 13.769 (9), 14.944 (13)
V (Å^3)	1529 (2)
Z	4
D_x (Mg m^{-3})	1.318
Radiation type	Mo $K\alpha$
No. of reflections for cell parameters	2240
θ range (°)	1.99–54.57
μ (mm^{-1})	0.09
Temperature (K)	25
Crystal form, color	Prism, colorless
Crystal size (mm)	0.5 × 0.35 × 0.35
Data collection	
Diffractometer	Bruker SMART Apex CCD detector on Huber four-circle
Data collection method	φ
Absorption correction	None
No. of measured, independent and observed reflections	67 606, 9984, 8069
Criterion for observed reflections	$I > 3\sigma(I)$
R_{int}	0.04
θ_{max} (°)	54.6
Range of h, k, l	$-16 \le h \le 17$ $-29 \le k \le 25$, $-33 \le l \le 33$
Refinement	
Refinement on	F
$R[F^2 > 2\sigma(F^2)]$, $wR(F)^2$, S	0.023, 0.020, 0.65
No. of reflections	8069
No. of parameters	682
H-atom treatment	Only displacement parameters refined
Weighting scheme	$w = 1/[\sigma^2(F_o)]$
$(\Delta/\sigma)_{max}$	<0.0001
$\Delta\rho_{max}$, $\Delta\rho_{min}$ (e Å^{-3})	0.22, −0.20

Computer programs used: *SMART*, *SAINT* (Bruker, 1997–2001; Koritsanszky *et al.*, 2003).

4. Results and discussion

4.1. Molecular and crystal structure

The molecular structure shown in Fig. 1 is very similar to that determined earlier by Bye (1976) at 298 K and needs no detailed discussion. The bond lengths and angles are similar to the values from the room-temperature measurement. It is, however, evident that the bond lengths at 25 K are 1% larger because of the reduced thermal motion. As expected, we observe a slight distortion of the aromatic ring *A* due to the strain in the molecule. C12 is displaced by 0.04 Å from the least-squares plane. This deviation disappears in molecules without the 4,5-ether bridge, such as dextromethorphan (Gylbert & Carlström, 1977). Rings *B* and *C* exhibit envelope conformers, whereas ring *D* shows a boat conformation. The piperidine ring (*E*) has the chair conformation found in all morphine-like molecules (see Table 2; Cremer & Pople, 1975; Luger & Bülow, 1983).

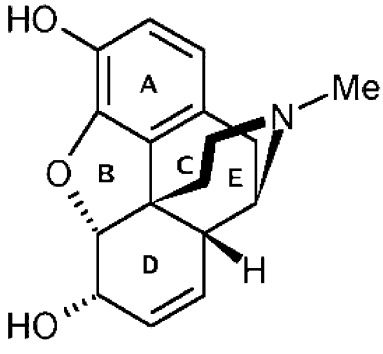

Figure 2
Definition of the rings in the oligocyclic structure of morphine.

Table 2
Ring puckering analysis.

Type: *E* = envelope, *C* = chair, *B* = boat.

Ring	Size	Q,q (Å)	Φ,φ_2 (°)	Θ (°)	Type
A	6	–	–	–	Planar
B	5	0.213 (5)	321 (1)	–	*E*†
C	6	0.559 (5)	117.8 (6)	126.0 (5)	*E*‡
D	6	0.573 (5)	70.8 (5)	94.4 (5)	*B*§
E	6	0.618 (5)	98 (3)	9.0 (4)	C

† C5 out of the plane. ‡ C14 out of the plane. § $B_{C6,C14}$.

4.2. Charge density and topological analysis

A quantitative comparison of the covalent bond strength can be given in terms of the bond topological properties. In Table 3 the values of the charge density and the Laplacian at the bond critical points (b.c.p.'s) are given. As expected, the

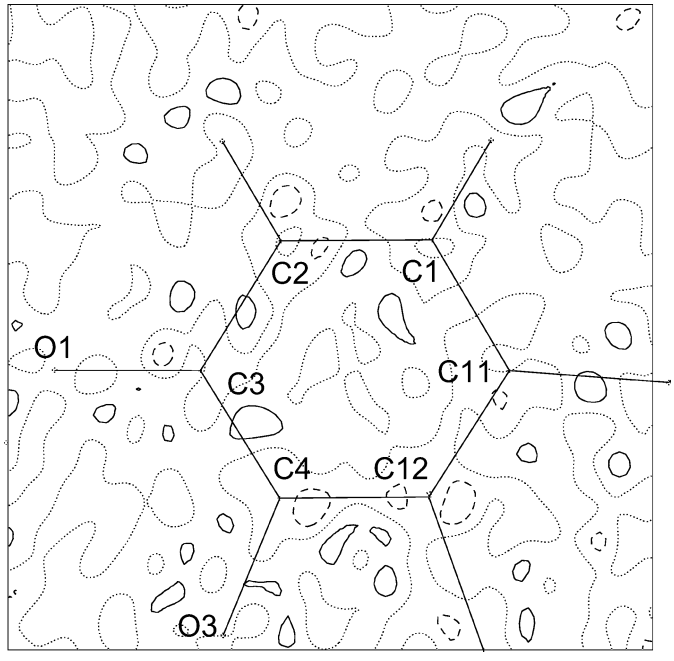

Figure 3
Residual map in the plane of the phenyl ring. Positive, negative and zero contours are represented by solid, dotted and dashed lines, respectively. Contour intervals at 0.1 e Å^{-3}.

Table 3
Bond and ring topological properties of morphine hydrate.

l = bond length in Å.

Bond	$\rho(\mathbf{r}_{bcp})$ (e Å^{-3})	$\nabla^2\rho(\mathbf{r}_{bcp})$ (e Å^{-5})	ϵ	Bond	$\rho(\mathbf{r}_{bcp})$	$\nabla^2\rho(\mathbf{r}_{bcp})$	ϵ
O1—C3	1.94	−12.1	0.05	C5—C6	1.62	−13.2	0.03
l = 1.3697 (6)	2.23 (5)	−22.3 (2)	0.12	l = 1.5629 (6)	1.65 (4)	−9.9 (1)	0.08
O2—C6	1.72	−13.7	0.09	C6—C7	1.73	−15.3	0.07
l = 1.4307 (6)	1.85 (5)	−10.6 (2)	0.05	l = 1.5169 (6)	1.84 (4)	−13.3 (1)	0.18
O3—C4	1.89	−13.7	0.04	C7—C8	2.29	−24.3	0.35
l = 1.3916 (6)	2.15 (5)	−14.9 (2)	0.04	l = 1.3530 (6)	2.50 (5)	−25.0 (1)	0.30
O3—C5	1.59	−11.9	0.02	C8—C14	1.71	−14.9	0.04
l = 1.4705 (6)	1.68 (4)	−6.8 (1)	0.03	l = 1.5122 (6)	1.75 (4)	−11.1 (2)	0.12
N1—C9	1.72	−15.0	0.04	C9—C14	1.57	−12.3	0.03
l = 1.4935 (6)	1.83 (4)	−10.8 (2)	0.20	l = 1.5646 (6)	1.71 (3)	−11.1 (1)	0.12
N1—C16	1.74	−15.4	0.07	C9—C10	1.56	−12.0	0.01
l = 1.4865 (6)	1.85 (4)	−9.4 (2)	0.12	l = 1.5669 (6)	1.57 (4)	−7.7 (2)	0.02
N1—C17	1.73	−15.2	0.05	C10—C11	1.68	−14.3	0.04
l = 1.4864 (6)	1.78 (4)	−10.1 (2)	0.18	l = 1.5202 (6)	1.68 (4)	−9.8 (1)	0.03
C1—C2	2.04	−20.2	0.22	C5—13	1.56	−12.0	0.01
l = 1.4115 (6)	2.14 (4)	−16.2 (2)	0.10	l = 1.5727 (6)	1.65 (4)	−9.8 (1)	0.17
C2—C3	2.01	−19.6	0.25	C12—C13	1.71	−14.4	0.03
l = 1.4242 (6)	2.11 (4)	−18.0 (2)	0.18	l = 1.5178 (6)	1.72 (4)	−9.4 (2)	0.02
C3—C4	2.13	−22.1	0.31	C13—C14	1.59	−12.4	0.01
l = 1.4016 (6)	2.24 (4)	−21.1 (2)	0.36	l = 1.5524 (5)	1.64 (4)	−9.4 (1)	0.13
C4—C12	2.16	−22.7	0.23	C13—C15	1.61	−13.0	0.01
l = 1.3921 (6)	2.27 (4)	−20.3 (2)	0.23	l = 1.5451 (6)	1.68 (4)	−10.6 (1)	0.09
C12—C11	2.09	−21.1	0.32	C15—C16	1.61	−13.2	0.02
l = 1.4009 (6)	2.19 (4)	−18.2 (2)	0.15	l = 1.5456 (7)	1.75 (4)	−11.8 (1)	0.09
C11—C1	2.04	−20.2	0.21				
l = 1.4160 (6)	2.20 (5)	−17.2 (2)	0.13				
6 ring *A*	0.14	3.5		5 ring *B*	0.30	6.3	
	0.18 (1)	3.1 (1)			0.40 (1)	5.2 (1)	
6 ring *C*	0.13	2.7		6 ring *D*	0.13	2.8	
	0.19 (1)	2.4 (1)			0.16 (1)	2.3 (1)	
6 ring *E*	0.13	2.7					
	0.16 (1)	2.2 (1)					

First line: values from a theoretical B3LYP/6-311++G(3df,3pd) calculation based on experimental geometry; second line: experimental results. The R values discussed in §4.1 are defined as: $R_p = \Sigma|\rho(\mathbf{r}_{bcp})_{exp} - \rho(\mathbf{r}_{bcp})_{th}|/\Sigma\rho(\mathbf{r}_{bcp})_{exp}$. $R\nabla^2 = \Sigma|\nabla^2\rho(\mathbf{r}_{bcp})_{exp} - \nabla^2\rho(\mathbf{r}_{bcp})_{th}|/\Sigma\nabla^2\rho(\mathbf{r}_{bcp})_{exp}$.

C7=C8 double bond has the highest $\rho(\mathbf{r}_{bcp})$ value of 2.50 (5) e Å^{-3}. The aromatic bonds have an average value of $\rho(\mathbf{r}_{bcp})$ = 2.19 (5) e Å^{-3}. This is in close agreement with our study of strychnine (Messerschmidt *et al.*, 2005), where $\rho(\mathbf{r}_{bcp})$ = 2.22 (11) e Å^{-3} was found for the aromatic bonds. For the 11 formal single bonds the $\rho(\mathbf{r}_{bcp})$ values range from 1.57 to 1.84 e Å^{-3} [average 1.69 (7) e Å^{-3}], which are also in line with the values found in the oligocyclic strychnine molecule. For the C—O(H) bonds the stronger bond (C3—O1) is next to the aromatic ring, while for C6—O2 the value of the electron density at the bond critical point is smaller. The C—N bonds are almost equivalent [1.87 (3) e Å^{-3}]. If the theoretical and experimental bond topological properties are compared for the 25 non-hydrogen bonds listed in Table 3, an average difference of 0.11 e Å^{-3} for $\rho(\mathbf{r}_{bcp})$ and 3.3 e Å^{-5} for $\nabla^2\rho(\mathbf{r}_{bcp})$ is found. These differences reduce to 0.09 e Å^{-3} and 2.7 e Å^{-5} if only the 18 C—C bonds are considered. If a relative agreement between experiment and theory is considered in terms of a reliability factor (defined as analogous to the conventional R value, see Table 3) $R\rho$ = 0.055 and $R\nabla^2$ = 0.25 are obtained. It is interesting to note that in our previous study on strychnine these discrepancies between experiment and theory were found to be 0.047 for $R\rho$ and 0.22 for $R\nabla^2$. Since in this case the experimental contributions were the average from four measurements it makes sense that for the present morphine study with only one experiment contributing to the R value calculation that these quantities are slightly larger. In total it can be confirmed again (Messerschmidt *et al.*, 2005) that the density uncertainty can be estimated to be around 5%, while for the Laplacian the standard uncertainly is much larger.

Additionally five ring critical points were located in the centers of the rings, which fit well with the theoretical values.

The topological values for the weak interactions are summarized in Table 4. As already mentioned by Bye (1976), there is a rather strong O—H···N interaction which links the molecules in chains along the *b* axis. The short $D\cdots A$ distance of 2.6352 (7) Å and the high density [0.30 (4) e Å^3] at the critical point support the strong character of this hydrogen bond. The water molecule is a donor of two hydrogen bonds linking O1 and O2. The static deformation density in the plane of these two bonds (see Fig. 4) shows the typical charge concentrations of the accepting oxygen lone pairs in the direction of the donor H atoms. The fourth O—H···O hydrogen bond (O2–H21···O4) and one of the water hydrogen bonds (O4—H41···O2) can be considered to be of medium strength, while the second water hydrogen bond is among the weaker ones. The two C—H···O contacts are very weak (see Table 4). The $\rho(\mathbf{r}_{bcp})$ values given in Table 4 are in the range of the exponential correlations between topological parameters and distances in hydrogen bonds established in the literature (Espinosa, Lecomte & Molins, 1999; Espinosa, Souhassou *et al.*, 1999; Flaig *et al.*, 2002; Steiner, 2002).

4.3. Atomic volumes and charges

The zero-flux surfaces of the electron density gradient vector field $\nabla\rho(\mathbf{r})$ allow the partitioning of a molecule into submolecular fragments. To evaluate the atomic volumes and charges, the program *TOPXD* (Volkov *et al.*, 2000) was used. The results are summarized in Fig. 5 (numerical data have been deposited[1]). The volume derived from experimental

[1] Supplementary data for this paper are available from the IUCr electronic archives (Reference: LC5024). Services for accessing these data are described at the back of the journal.

Table 4
Intermolecular contacts indicating the possible hydrogen bonds and their bond topological parameters.

D—H $\cdots A$	$\rho(\mathbf{r}_{BCP})$ (e Å^{-3})	$\nabla^2\rho(\mathbf{r}_{BCP})$ (e Å^{-5})	H$\cdots A$ (Å)	$D\cdots A$ (Å)	D—H (Å)	D—H—A (°)
O1—H11$\cdots$N1^{i}	0.30 (4)	5.4 (1)	1.67	2.6352 (7)	0.97	
O2—H21$\cdots$O4^{ii}	0.19 (1)	4.7 (1)	1.74	2.7023 (8)	0.97	174
O4—H41$\cdots$O2^{iii}	0.19 (3)	1.3 (1)	1.83	2.7950 (8)	0.97	178
O4—H42$\cdots$O1^{iii}	0.13 (1)	0.4 (1)	2.00	2.9659 (8)	0.97	171
C8—H8$\cdots$O1^{iv}	0.06 (1)	1.2 (1)	2.27	3.1741 (7)	1.08	140
C9—H9$\cdots$O3^{v}	0.05 (1)	0.9 (1)	2.48	3.3199 (6)	1.08	134

Symmetry codes: (i) $2-x,\frac{1}{2}+y,\frac{1}{2}-z$; (ii) $\frac{1}{2}+x,\frac{3}{2}-y,1-z$; (iii) x,y,z; (iv) $1-x,-\frac{1}{2}+y,\frac{1}{2}-z$; (v) $2-x,-\frac{1}{2}+y,\frac{1}{2}-z$.

Table 5
Atomic properties of the CH_2/CH_3 groups (values in Å^3 and e, respectively).

	V_{001}		N_{001}	
Group	(exp.)	(th.) Matt	(exp.)	(th.)
$C10H_2$	19.57	21.37	7.66	7.90
$C15H_2$	21.98	21.38	7.85	7.88
$C16H_2$	21.79	20.27	7.80	7.55
$C17H_3$	25.55	28.54	8.28	8.39

densities (V_{tot}) is defined by the interatomic boundaries in the crystal, while V_{001} used in Fig. 5 describes a volume of an atom with a cutoff of ρ = 0.001 a.u., which is commonly used in theory. This cutoff is suited for an adequate comparison between theory and experiment. As the sum of the atomic charges is zero and the volumes (V_{tot}) multiplied by Z = 4 reproduce the unit-cell volume to within less than 1% (0.8%), the integration procedure can be considered to have worked properly.

The representation in Fig. 5 shows the volumes (upper part of Fig. 5) and electron populations (lower part) for the corresponding quantities of fragments 1–3, as defined in Fig. 1, and the Matta results (Matta, 2001) plotted *versus* the experimental morphine values. The correlation with a linear fit is 0.979 for the volumes and 0.998 for the electron populations. In addition to the least-squares lines, the bisecting lines are drawn in Fig. 5 to illustrate easily the agreement/disagreement between experiment and theory. As expected, the atomic properties of the calculated fragment molecules 1–3 fit well with the values of Matta (correlation coefficient of 0.988 for the volumes and 0.999 for the electronic populations; for a graphical representation see the supplementary material). Comparing experiment and theory some notable deviations from the bisecting line exist for the volumes. For the O atoms (volumes $>$ 13 Å^3) higher volumes are found from theory compared with the experimental values, while the electron populations are less affected.

The majority of the aliphatic carbon atoms (volumes 6–10 Å^3) are grouped below the bisector and a cluster of hydrogen volumes (volumes $<$ 6 Å^3) is seen above, indicating that the C atoms of predominantly methyl or methylene groups show an increased experimental volume, while the opposite is true for the H atoms.

The electron populations distribute rather closely to the bisector with a similar, but less pronounced, trend as observed for the volumes in that slightly higher experimental values for carbon are seen while again the opposite holds for the corresponding H atoms. These effects almost cancel each other out if entire CH_2 or CH_3 groups are considered rather than single atoms. As Table 5 shows, there is a good agreement (within less than 3%) between experimental and theoretical atomic properties of these groups, which is closer for the electron populations. An exception is the terminal methyl group $C17H_3$, where for the isolated molecule (in theory) a larger volume is allowed than in the (experimental) crystalline environment.

The discussion above suggests that the partitioning of the experimental electron density leads to polarized C—H bonds, while the theoretically derived C and H atoms are close to neutral. To some extent the discrepancies can be attributed to the limited 6-31G* basis set, which lacks polarization functions for the H atoms. However, as already mentioned, this basis set was used for a direct comparison with the theoretical results of Matta (2001).

5. Conclusions

In this study, a full topological analysis of the experimental charge density was performed on morphine hydrate. For $\rho(\mathbf{r}_{bcp})$ and $\nabla^2\rho(\mathbf{r}_{bcp})$ the experimental and theoretical values of the non-hydrogen bonds agree in the range 0.11 e Å^{-3} and

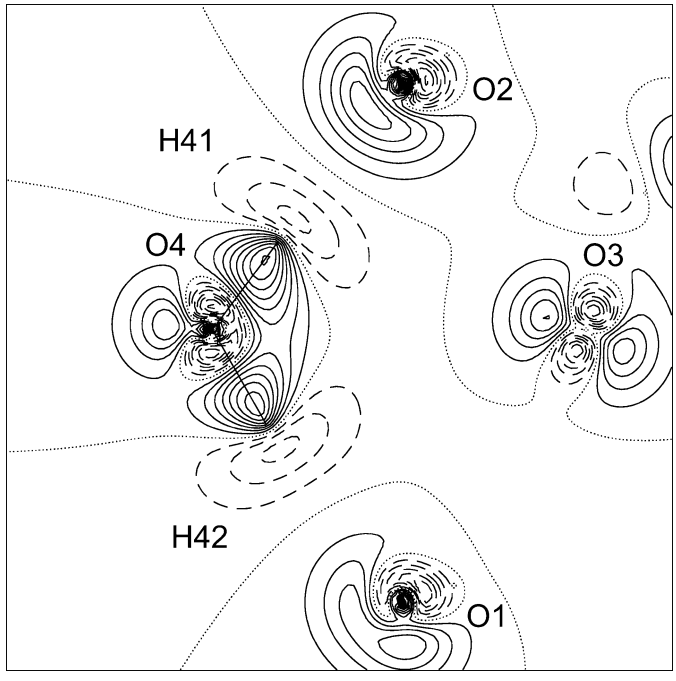

Figure 4
Static deformation density map in the plane of the two hydrogen bonds originating from the water molecules. Contour lines as in Fig. 3.

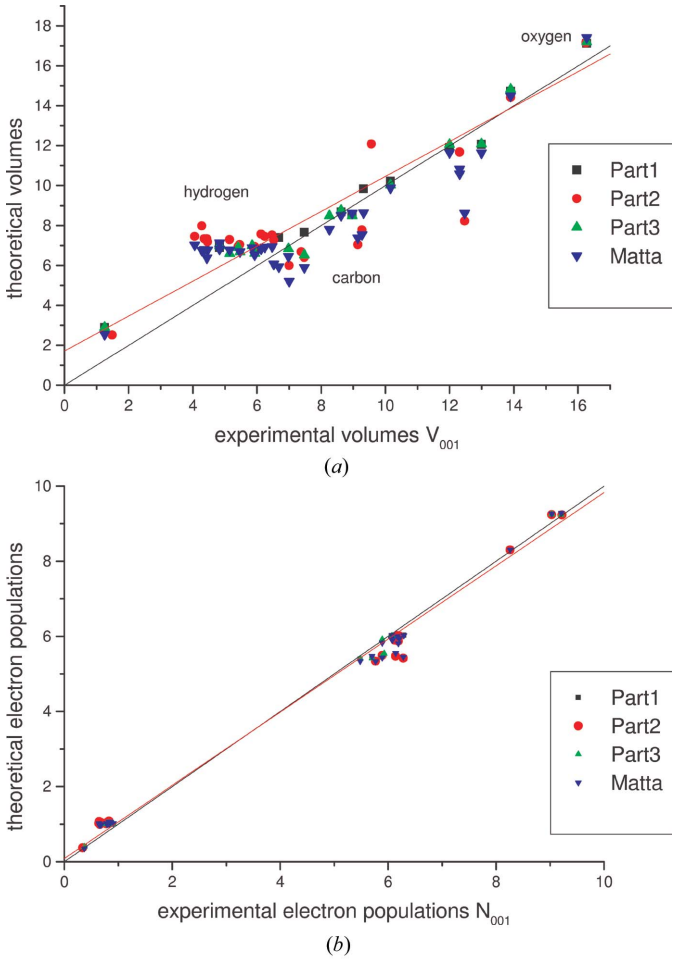

Figure 5
Representation of the theoretical *versus* experimental atomic properties. Above: volumes V_{001} (in Å^3); below: electron populations (in e). Least-squares line (red) and bisecting line (black) are also shown.

3.3 e Å^{-5}, which is in line with the previous findings of Flaig *et al.* (2002), Pichon-Pesme *et al.* (2000) and Messerschmidt *et al.* (2005).

The atomic volumes and charges obtained were compared on one hand with fragment molecules which allow the complete reconstruction of the morphine molecule, and on the other hand with Oripavine PEO, an opiate calculated by Matta. The values of the calculated fragments fit well with those from Matta. Comparing the experimental and theoretical atomic properties shows some differences. If CH_2 or CH_3 group properties for aliphatic C atoms are calculated rather than single atoms, these differences, caused mainly by polarized C—H bonds in the experimental density, almost cancel each other out.

This study will be continued with further morphine-like molecules to examine the impact of small chemical variations on the electron-density distribution which might help in understanding further the rather different physiological properties in this class of compounds.

References

Allen, F. H., Kennard, O., Watson, D., Brammer, L., Orpen, A. & Taylor, R. (1992). *International tables for Crystallography*, Vol. C, ch. 9.5, pp. 685–706. Amsterdam: Kluwer Academic Publishers.

Bader, R. F. W. (1994). *Atoms in Molecules. A Quantum Theory*, No. 22 in The International Series of Monographs on Chemistry, 2nd ed. Oxford: Clarendon Press.

Bruker AXS Inc. (1997–2001). *Programs ASTRO, SMART, SAINT*. Bruker AXS Inc., Madison, Wisconsin, USA.

Burnett, M. N. & Johnson, C. K. (1996). *ORTEP*III. Report ORNL-6895. Oak Ridge National Laboratory, Tennessee, USA.

Bye, E. (1976). *Acta Chem. Scand. B*, **30**, 549–554.

Cheeseman, J., Keith, T. A. & Bader, R. F. W. (1992). *AIMPAC Program Package*. McMaster University, Hamilton, Ontario.

Cremer, D. & Pople, J. (1975). *J. Am. Chem. Soc.* **97**, 1354–1358.

Espinosa, E., Lecomte, C. & Molins, E. (1999). *Chem. Phys. Lett.* **300**, 745–748.

Espinosa, E., Souhassou, M., Lachekar, H. & Lecomte, C. (1999). *Acta Cryst.* B**55**, 563–572.

Flaig, R., Koritsánszky, T., Dittrich, B., Wagner, A. & Luger, P. (2002). *J. Am. Chem. Soc.* **124**, 3407–3417.

Frisch, M. J. *et al.* (1998). *GAUSSIAN*98, Revision A.7. Gaussian Inc., Pittsburgh, PA, USA.

Gylbert, L. & Carlström, D. (1977). *Acta Cryst.* B**33**, 2833–2837.

Hansen, N. K. & Coppens, P. (1978). *Acta Cryst.* A**34**, 909–921.

Koritsánszky, T., Richter, T., Macci, P., Gatti, C., Howard, S., Mallinson, P. R., Farrugia, L., Su, Z. W. & Hansen, N. K. (2003). *XD*. Freie Universitaï, Berlin, Germany.

Luger, P. & Bülow, R. (1983). *J. Appl. Cryst.* **16**, 431–432.

Matta, C. F. (2001). *J. Phys. Chem. A*, **105**, 11088–11101.

Meserschmidt, M., Meyer, M. & Luger, P. (2003). *J. Appl. Cryst.* **36**, 1452–1454.

Messerschmidt, M., Scheins, S. & Luger, P. (2005). *Acta Cryst.* B**61**, 115–121.

Pichon-Pesme, V., Lachekar, H., Souhassou, M. & Lecomte, C. (2000). *Acta Cryst.* B**56**, 728–737.

Popelier, P. & Bone, R. (1998). Local prgram. UMIST, Manchester, UK.

Sheldrick, G. M. (1997). *SHELXL*. University of Göttingen, Germany.

Steiner, G. M. (2002). *Ang. Chem. Int. Ed.* **41**, 48–76.

Volkov, A., Gatti, C., Abramov, Y. & Coppens, P. (2000). *Acta Cryst.* A**56**, 252–258.